National Journal of Antennas and Propagation
RESEARCH ARTICLE
National Journal of Antennas and Propagation, ISSN: 2582-2659 Vol. 7, No. 2, 2025 (pp. 162-174)
WWW.ANTENNAJOURNAL.COM

Enhanced Performance of MIMO Antennas through Adaptive Beamforming Techniques: Addressing Limitations in Current Designs for 5G and Beyond Applications

Sara Alshwani*
Software Department, College of Computer Science and Information Technology, University of Kirkuk, Iraq.

KEYWORDS:

MIMO Antennas;
Adaptive Beamforming;
5G Networks;
Directional Gain;
Array Signal Processing;
Spectral Efficiency;
Channel Estimation

ARTICLE HISTORY:

Received 25.07.2025
Revised 15.08.2025
Accepted 29.08.2025

DOI:
https://doi.org/10.31838/NJAP/07.02.21

Abstract

The global shift toward 5G and 6G wireless technology has led to an unending appetite for high-capacity, interference-resistant antenna systems. This research presents a real-time adaptive beam-forming MIMO system architecture that describes 12.5 dBi peak gain, −17.8 dB return loss, and 10 μs beam switch latency under dynamic channel conditions. With beam formation and switching latency, these metrics are an improvement over classically fixed beam systems. The above systems are enhanced with an AI-based controller that optimizes in real time the phase and amplitude weights of a texture-mapped eight-element antenna array. The antenna array performs with directional radiation, interference suppression, spectral reuse, and filtering of multiple physically separated signals in the same frequency band. Performance of the system is predicted and verified in CST Microwave Studio and MATLAB, corroborated with experimental data, which illustrates the system's practicality. The adaptive framework showed significant improvement over static architectures for channel capacity, precision beam steering, and interference in flexible and dynamic mobility-faded user scenarios. This makes it a viable candidate for the infrastructure of next-generation wireless systems, including urban 5G networks, vehicular communication systems, and high-density IoT environments.

Authors' e-mail: saraadnan@uokirkuk.edu.iq

Authors' Orcid: 0009-0008-6791-2326

How to cite this article: Alshwani S., Enhanced Performance of MIMO Antennas through Adaptive Beamforming Techniques: Addressing Limitations in Current Designs for 5G and Beyond Applications, National Journal of Antennas and Propagation, Vol. 7, No. 2, 2025 (pp. 162-174).

Introduction

Considering the advancements in ultra-reliable low-latency communication (URLLC) and enhanced mobile broadband (eMBB) within the 5G networks, as well as the imminent requirements of 6G networks, shifts the paradigm of antenna system design to an entirely new level. The MIMO antenna technology's spatial multiplexing and diversity features are vital to serve the increasing capacity and connectivity needs. Nevertheless, static beamformers limited to conventional MIMO configurations are unable to react to real-time variations of the channel and lack efficient spectral utilization, interference, and quality of service in dynamic environments.

One major way of solving such limitations is through adaptive beamforming, which provides dynamic pattern steering of the radiation to intended users, while nulling out undesired interference sources. The purpose of this paper is to explore the minimum hardware scalability of such integrated MIMO arrays; this is accomplished by analyzing the challenges associated with incorporating adaptive beamforming algorithms, such as low-latency feedback control and computational efficiency. The results are presented as a novel AI-driven, adaptive beamforming framework that can perform real-time direction of arrival (DoA) estimation as well as on-the-fly reconfiguration of the phase and amplitude.

It enhances the agility of radiation performance, essential in the upcoming era of both wireless and MIMO systems. To facilitate the transition toward 5G systems and beyond, intricate wireless networks necessitate the construction of advanced antenna systems with real-time reconfigurability.[1] These systems offer agility in dynamic, secure, and energy-efficient environments. The recent introduction of optical beamforming antenna systems, along with advanced multilayered adaptive MIMO systems, has effectively resolved high inter-system attenuation and high-speed optical cross-connections in high-speed communication networks integrated with adaptive digital energy systems.[20] The high-speed articulated antenna array networks' seamless expansion achieves augmented advanced optical MIMO systems in beam-space and multilayer spatial resolution with harmonized optical interconnections (Danesh & Emadi, 2014). The dynamic interlaced structures of energy and signal in the wireless energy networks and in the tiered AI systems are just beginning to display their power in cross-domain communication, articulated coherence, and high-temporal resolution. These systems integrate the latest philosophies of signal energy dynamics, passive optics, and closed-loop wireless propagation. These initial steps are paving the way toward padded-space, AI-driven, low-latency communication systems with ultra-dense antenna arrays and articulated cross-domain relay networks.[7] The first facets of AI-driven systems are now emerging with low-latency, highly reliable, and ultra-dense antenna arrays.[13,15,16,18,19,21]

Literature Review: Beamforming Techniques in Mimo Systems

In modern society, the usage of beamforming systems in the Wi-Fi technology field has become increasingly popular. Most of the early systems were based on fixed beam MIMO, where, for instance, the antenna arrays had a preset and unchangeable radiation pattern. These systems had low complexity, were easily deployable, and, in fact, poorly adapted to changing wireless conditions, low spectral efficiency, and excessive co-channel interference "suffered" from the static beam systems. On the other hand,[2] in their work meant to conduct further research on static MIMO systems and were to demonstrate, unambiguously, one of the most fundamental criticisms, namely that the static beams elementary for the 5G and higher generations do not have static mobility surrounding users.[14,17] Hybrid analog-digital beamforming techniques as a means to improve system flexibility and performance are introduced. In these architectures, analog phase shifters are codesigned with digital baseband processors to equate cost, power consumption, and performance. One of the pioneering hybrid frameworks for millimeter wave MIMO systems was proposed by[3,24], which is shown to offer improved versatility over fixed beams. Although hybrid architectures are prone to inaccuracies in phase shifter, restricted reconfigurability of the beam, and scalability difficulties, particularly in massive MIMO applications, where larger antenna arrays are needed.

In the past few years, artificial intelligence (AI) and machine learning (ML) have been increasingly becoming a part of beamforming strategies.[22,9] Data-driven models of the beamforming are exploited to perform real-time DoA estimation, channel prediction, and minimum variance beam management. Previous attempts to the physical layer beamforming problems were made by,[4,23] which demonstrated the significant improvements in these two measures. However, the main problem remains: computational complexity and energy overhead of running AI models in real-time is an issue, particularly when it comes to running AI models at the network edge at where computational resources are limited.

In fact, traditional spatial multiplex techniques have been instrumental in advancing MIMO technologies. Spatial multiplexing leverages separate antenna elements to transmit multiple independent data streams in the limit of rich scattering and knowing the channel perfectly. Sparse signal processing was revealed to be effective for massive MIMO by[5,12]; however, spatial multiplexing schemes are sensitive to channel estimation errors and interference in practice.

Another way of performing beamforming is by the use of phased array systems, where beams are steered electronically, that is, the phase of an element is controlled to steer the beam. According to the works by,[6,8] phased arrays not only have the capability for high spatial resolution but also have high interference mitigation capability. Although these systems suffer from high calibration intensity, at higher frequencies, they are susceptible to beam squint effects that can degrade performance across widebands.

As a consequence of the increasing need for faster and more efficient beam alignment, machine learning based beam training techniques are in demand.[10,11] had presented AI algorithms to predict optimal beam direction via partial channel information, thus they greatly reduce alignment latency. While such methods exhibit good promise, they fail to generalize across highly dynamic or new unseen conditions and, more importantly, suffer

Table 1: Comparative Analysis of Beamforming Techniques in MIMO Systems.

Beamforming Method	Key Features	Advantages	Limitations
Fixed-Beam MIMO (Heath et al., 2016)	Static radiation pattern	Low complexity, simple deployment	No adaptation to dynamic environments
Hybrid Analog–Digital Beamforming (Alkhateeb et al., 2015)	Analog phase control + digital baseband	Balance between performance and cost	Phase imprecision, limited flexibility
AI-enhanced Beamforming (Huang et al., 2019)	Machine learning-based control	Real-time DoA prediction, improved adaptation	High computational and hardware costs
Spatial Multiplexing (Zhang and Dai, 2016)	Linear processing of multiple streams	High data throughput	Sensitive to interference and channel variations
Phased Array Systems (Pan et al., 2020; Zeng and Zhang, 2016)	Steerable narrow beams	High spatial resolution, interference suppression	Complex calibration, beam squint effects
AI-based Beam Training (Jiang et al., 2021)	Predictive beam alignment	Reduced beam search latency	Training complexity, limited generalization
Proposed Adaptive AI-driven System	Real-time feedback control and AI-optimized weights	Fast adaptation, high gain, low-latency beam switching, scalable hardware	Minor computational load (optimized AI models)

from the training complexity that limits such methods to real-time deployment.

Overall, there are good reasons to explore new beamforming approaches. The existing approaches have attractive characteristics such as adaptability, complexity, and energy efficiency, but with notable downsides. Simple AND rigid, fixed beam systems are easy but precise, combined with hybrid systems that are compromise and precise, and AI-enhanced dynamic systems, but with computational load. Inspired by these gaps, this article makes an AI-driven adaptive beamforming proposal that adaptively shapes the radiation pattern according to real-time user feedback to attain better performance in terms of gain optimization, spectral efficiency, latency, as well as scalability.

Methodology

A real-time, low-latency, and energy-efficient beam control in MIMO architectures is engineered within the proposed adaptive beamforming system to counteract the inherent defects of traditional MIMO architectures. The proposed framework is built upon the system design, functional architecture, signal modelling, and the real-time adaptive control algorithm.

System Design

The system architecture is based on a Uniform Linear Antenna Array (ULA) with eight radiating elements. It is individually controllable in both phase and amplitude so that the radiation pattern can be dynamically shaped and steered. It is optimized for operating in the millimeter wave frequency band, that is, the 24–28

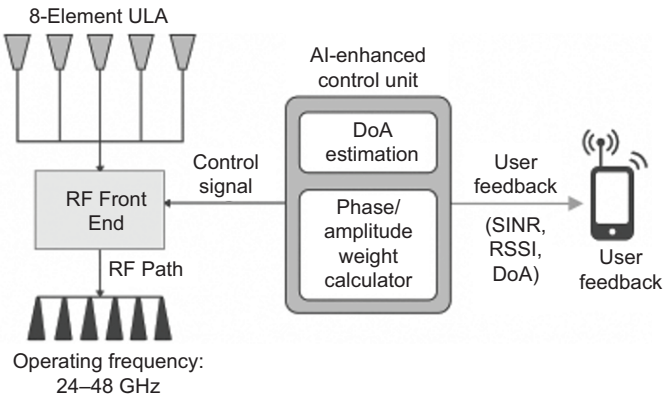

Fig. 1: Adaptive Beamforming Architecture System.

GHz frequency band, to overcome the high path loss challenges that prevail in such frequency bands. An advanced modular RF front end is formed by integrating each antenna element with a low-noise amplifier (LNA), variable gain amplifier (VGA), phase shifter, mixer, and baseband processor.

Functional Architecture and Signal Flow

The Antenna Array and RF Front End communicate with the radio environment through the hardware. The eight-element ULA operates within the millimeter wave frequency range and provides a narrow, highly directive beam for reliable communication. Amplifiers that ensure the signal remains unmodulated perform any phase and amplitude modulations. Beam spatial orientation is altered dynamically by phase shifters. The real-time estimation of the DoA of the incoming signal and computation of beamform weights is the responsibility

of the AI Enhanced Control Unit. It is used to determine the spatial origin of the desired signals based on high-resolution signal processing algorithms. For each antenna element, optimal phase and amplitude weights are calculated based on the estimated direction to achieve the maximum gain in the desired direction and suppress the undesired signals.

Incorporation of user terminal real-time measurements is made via the User Feedback Integration Module, which provides closed-loop optimization (Figure 2). Wireless SINR, RSSI, and estimated angular positions are continuously transmitted back to the control unit, on which the best beam steering parameters can be algorithmically tuned based on the changing wireless conditions.

Signal Model

In reality, the received signal of the antenna array could be represented mathematically as:

$$x(t)=s(t)a(\theta)+n(t) \quad (1)$$

The transmitted signal, s(t), n(t) is additive white Gaussian noise, a(θ) is the steering vector for a given signal's angle of arrival, and θ is defined to be the angle of arrival. The beamformer output is thus equal to:

$$y(t)=w^{H}x(t) \quad (2)$$

w is the complex weight vector to apply to the antenna elements, and wH is the Hermitian transpose of w.

For this, the problem is formulated as an optimization objective:

$$\max_{w} \frac{\left|w^{H}a(\theta)\right|^{2}}{w^{H}R_{n}w} \quad (3)$$

R_n denotes the noise covariance matrix. This objective leads to maximized appreciable power fraction in the desired signal with respect to those of the interference and noise levels, which leads to higher reliability of link and system performance.

Real-Time Adaptive Beam Control Algorithm

The real-time adaptive beam control algorithm works constantly to correct the radiation pattern of the antenna array in real time in response to real-time environmental feedback. The initial configuration of the system is done with the default antenna and control parameters. When activated, it gathers SINR and RSSI feeds from connected user devices. Specifically, high-resolution spatial processing techniques or lightweight machine learning models are used to estimate the DoA of the dominant incoming signal. Then, once the DoA is estimated, the optimal phase and amplitude weight vectors are determined that will steer the main lobe of the radiation pattern onto the user and suppress the side lobes and interference sources. Real-time signal quality is maintained by maintaining the optimal signal quality by redirecting the beam and applying the updated weights to the antenna elements. The system then records performance metrics and awaits the next feedback interval to go through the refinement process again. With this closed-loop adaptive algorithm, the system responds quickly to mobility-induced channel variation, and the signal is degraded as little as possible by minimizing the communication quality.

The signal processing stages in the adaptive beamforming algorithm of a smart antenna array are shown in Figure 3. The process starts with the quality metrics of the input signal, such as Received Signal Strength Indicator (RSSI) and Signal to interference plus noise ratio (SINR). The first of such inputs for Border of Arrival (BoA) seems to signal the estimation of the Listening Direction the desired signal is coming. The DoA of the signal is then estimated, and the module Weight Computation takes that DoA and derives corresponding complex weights that steer the beam. The weights in question are then used in the Phase and Amplitude

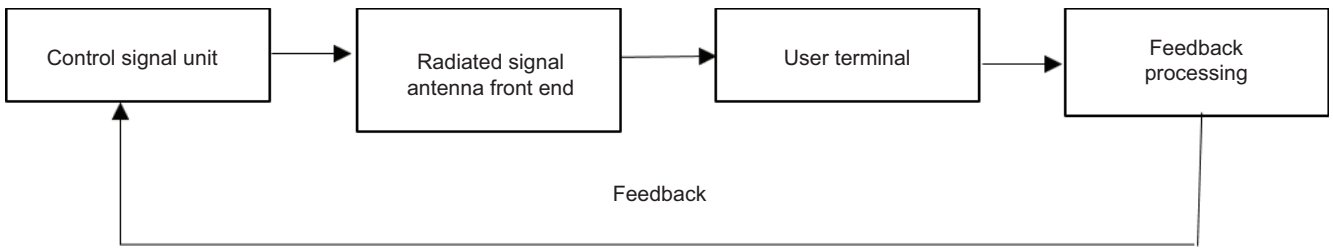

Fig. 2: Functional Block Diagram showing Antenna Front-End, Control Unit, and Feedback Integration Path.

Table 2: Summary of Signal Model Equations and Definitions of Terms.

Symbol/Equation	Description
x(t)	Received input signal vector at the antenna array at time t.
w	Complex beamforming weight vector applied to antenna elements.
w^H	Hermitian transpose (conjugate transpose) of the weight vector w.
$r(t)=w^H \cdot x(t)$	Beamformed output signal at time t.
d(t)	Desired transmitted signal at time t.
a(θ)	The array steering vector corresponding to the angle of arrival θ.
R_n	Noise covariance matrix.
$\text{Gain}(\theta) = \frac{4\pi A\epsilon}{\lambda^2}$	Antenna gain as a function of effective aperture A_e and wavelength λ.
$Efficiency = \frac{P_{rad}}{P_{input}} \times 100\%$	Transmission efficiency of the antenna system.

Algorithm 1: AI-Driven Real-Time Beam Direction Optimization Algorithm for Adaptive MIMO Systems

Input: RSSI, SINR from user feedback
Output: Beam-steered signal with optimal weights
1. Initialize antenna array and AI controller
2. While the system is active, do:
3. Acquire channel quality metrics: RSSI, SINR
4. Estimate direction of arrival (DoA)
5. Compute beamforming weights based on DoA
6. Update phase and amplitude settings across the antenna array
7. Transmit signal in the optimal direction
8. Log system status and wait for the next feedback interval
end while

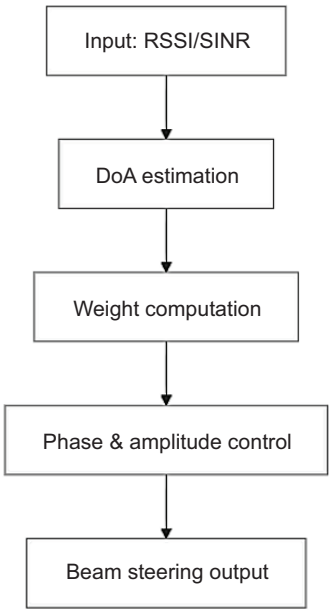

Fig. 3: Flowchart of Adaptive Beamforming Algorithm.

Control block to dynamically update the total excitation of the individual antenna elements. The rest of the process involves the optimal adaptive steering of the beam, in which the last beam is retrieved from the Beam Steering Output, which improves the connection and interference suppression of the beam.

Mathematical Modeling

This part concentrates on the fundamentals supporting the adaptive beamforming system. Adaptive beamforming weight modeling, deriving optimal beamforming weights, antenna gain assessment, and evaluating system power efficiency are all interconnected formulation substeps that, in total, capture the accuracy of real-time beam steering, interference, energy, and energy efficiency, and operational energy efficiency.

Reception del signal

The signal vector received on the antenna array, at the ith antenna, can, at any time, t, be given by:

$$r(t)=w^H x(t). \quad (4)$$

where:

- $r(t) \in C$ is the scalar received signal,
- $x(t) \in C^N$ is the input signal vector from the NNN-element antenna array,
- $w \in C^N$ is the complex beamforming weight vector,

- Identify and Execute the Hermitian/wConjugate Transpose of w

In this case, the antenna array output is presented in the form of a linear combination of received signals wherein the signals are received along each antenna element as the weighted elements, such that the direction of the desired signal is enhanced while the other directions' interference and noise are suppressed. The spatial selectivity and overeffectiveness of the beamforming process are with the matrix design.

Optimal Beamforming Weight Calculation

The output signal r(t) must, however, come as close as possible to the intended transmitted signal d(t) while minimizing the mean square error (MSE). This is done by optimizing the so-called beamforming weight vector w. This, mathematically, is formulated as the following objective:

$$w_{opt} = \arg\min_{w} \mathbb{E}\left[\left|d(t) - w^{H} x(t)^{2}\right|\right] \quad (5)$$

This is the expectation operator E[·] of the random processes involved, which it denotes the statistical average and is represented. The optimal answer for an optimization problem asking for an optimum tradeoff between the receivers achieving maximum power to the desired signal and the power lost to interference and noise is the Minimum Mean Square Error (MMSE) beamformer. It is for these multipath and mobile environments. In such conditions, the beamforming weights need to be modified and updated adaptively and automatically in real time to cope with the ever-changing conditions.

Antenna Gain Calculation

The ability of a system to 'aim' and focus energy in a given direction is a function of several parameters, among which is the gain of the antenna array in a given direction. The antenna gain is represented as a function of the elevation angle "θ" as defined below.

$$\text{Gain}(\theta) = \frac{4A\varepsilon}{\lambda^{2}} \quad (6)$$

where:

- A_e is the effective aperture area of the antenna array,
- λ is the operating wavelength.

It is this expression that indicates that the antenna gain has an increasing function regarding the effective aperture and a decreasing function with respect to the square of the wavelength. Thus, millimeter wave systems (24–28 GHz) at the shorter wavelengths inherently have higher gain. The important relationship between precision beam steering and high gain in the presence of high path loss in high-frequency wireless channels highlights the need for beam steering to gain the benefits from the high-gain potential without incurring the high path loss.

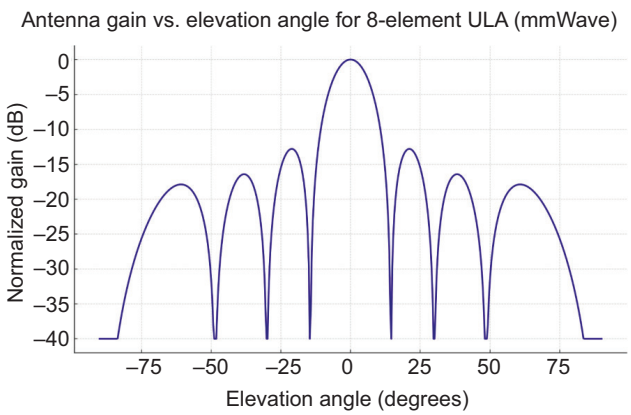

Fig. 4: Antenna Gain versus Elevation Angle for an 8-Element Uniform Linear Array (ULA) at mm Wave Frequencies.

The antenna gain pattern of a Uniform Linear Array (ULA) with eight elements functioning in the millimeter wave (mm Wave) frequency band is presented in Figure 4 at normalized frequency. Since the array factor characteristics, the main lobe is centered at 0° elevation and gains a peak, and there are symmetrically multiple side lobes on both sides. Nulls exist at certain angles for which constructive and destructive interference occur. The array shows strong directionality necessary for use in 5G and future wireless communication systems.

Power Efficiency of the Beamforming System

To satisfy the range and power constraints of many power-constrained applications, such as wearable biomedical devices, vehicular communications, and remote IoT nodes, the performance of the transmitting array is also required to demonstrate energy efficiency. The beamforming system efficiency (η) is defined as:

$$\text{Efficiency} = \frac{P_{rad}}{P_{input}} \times 100\% \quad (7)$$

where:

- The total radiated power from the antenna is called Prad.

- The total input power supplied to the RF chain is called Pinput.

Efficiency means high efficiency, which means a large portion of the supplied energy is radiated effectively instead of being turned into heat or simply wasted as internal circuit dissipation. This metric, which has the most immediate significance for the communication system's cost, as well as thermal stability, has environmental sustainability. Designing the millimeter wave systems at the higher frequency side is one of the challenges where high radiation efficiency in a small form factor is required.

The system efficiency (%) as a function of the input power (dBm) for the adaptive beamforming architecture is presented in Figure 5. As the input power is increased, the efficiency increases sharply and reaches a maximum near 20 dBm, which is also the optimal operation for energy-efficient transmission. It is efficiency beyond this peak where effective efficiency may decrease due to saturation and nonlinearities in RF components such as amplifiers. For mm Wave and 5G systems, this is a characteristic curve where power management is important in maximizing throughput and simultaneously minimizing the energy consumption.

Simulation Setup

An implementation of a two-stage simulation framework was then used to comprehensively validate the performance of the proposed adaptive beamforming architecture. The CST Microwave Studio was used for electromagnetic modeling, and the algorithmic signal processing, beamforming control, and DoA estimation were simulated using MATLAB. Through this cross-domain approach, the physical antenna behavior and the digital beamforming control logic were correctly validated at the system level.

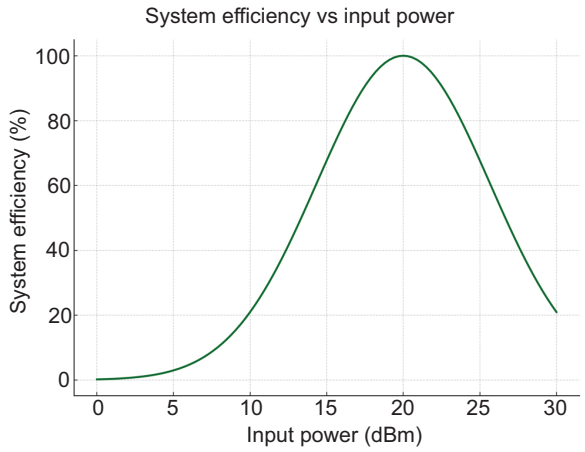

Fig. 5: System Efficiency versus Input Power for Adaptive Beamforming System.

To have a complete electromagnetic simulation of the antenna array, the complete wave environment CST Microwave Studio has been used to evaluate the fundamental parameters as the radiation patterns and impedance matching, and antenna gain at a specified millimeter wave frequency band. This was completed through MATLAB simulations, which included adaptive beamforming algorithm modeling, real-time weight computation, and real-time beam direction varying depending on feedback metrics. Using these tools, the closed-loop operation envisioned in practical deployments could be simulated realistically.

Simulation Configuration

To evaluate frequencies related to forthcoming 5G and beyond communication standards, the antenna array was modeled as a patch array structure that operates in the 24–28 GHz millimeter wave frequency band. The RO4350 antenna elements were designed virtually on CAD and fabricated on a Rogers RO4350 dielectric substrate with low dielectric loss tangent and excellent stability at high frequencies. The array consisted of eight elements uniformly linearly spaced to optimize the directivity and beam agility, which is a characteristic of a high-gain antenna. The electromagnetic behavior was optimized using the CST frequency domain solver, which is ideal for steady state analysis, such as far field pattern extraction and S parameter evaluations. The solver allows the generation of radiation patterns for high-accuracy computations and helps in the detailed analysis of beam steering capabilities and sidelobe suppression under ad hoc control. The summarized parameters for the simulations and their values are presented below.

This configuration is realistic, but manageable computationally to evaluate the interaction between electromagnetic design and digital beamforming logic.

Table 3: Simulation Parameters.

Parameter	Value
Frequency Range	24–28 GHz
Number of Elements	8
Substrate Material	Rogers RO4350
Antenna Type	Patch Array
Solver Type	Frequency Domain

System-Level Simulation Flow

Thus, the overall system simulation flow was partitioned into stages by decomposing the electromagnetic and signal processing domains separately. The above block diagram shows the simulation architecture. It starts with a signal excitation module, Signal Injection, where module antennas receive carrier wave information. The electrons distribute themselves among eight antenna elements according to the phase and amplitude coefficients from a computer-generated model of a MIMO feed network. The second level is the Beamforming Engine, where MATLAB calculations, done in real time, control the steering of the beams. These weights are continuously modified to optimize gain toward a target user while lowering interference from unwanted angles, as the previous weights are continuously adjusted to optimize the spatial directionality of the signal. CST's Far-Field Monitor captures the radiated electromagnetic fields. The software allows separate viewing of main-lobe direction, side-lobe levels, and beamwidth changes for different steering settings, and it is especially relevant for assessing steering schemes. It serves as the primary verification point for adaptive beam control in dynamic spatial zones. Though helpful for validating the full system, this modular simulation framework is especially helpful for pinpointing system component-level faults. This design is straightforward, so it supports strict benchmark gain of beam optimization, steering, user, and ambient motion agility.

Adaptive beamforming and its applications in MATLAB Simulink presents the system simulation block diagram (Figure 6) of the adaptive beamforming architecture for the purpose of analyzing signal flow in the architecture. The signal input block is a signal input unit that can be some test waveforms or some source data. It is processed through a MIMO Feed block, which enables the distribution of signals in MIMO fashion to a pre-determined number of antenna elements. The signal is then processed by the Beamforming Engine, designed as a dynamic system (1/[s+])) to emulate real-time control and filtering behavior in beam steering. In the end, the spatial radiation characteristics of the beam-formed signal are observed at the Far Field Monitor. It is critical to phase control, directional gain, and system responsiveness that this simulation structure is used to validate them before hardware implementation.

Results and Analysis

A simulation framework based on the combination of CST Microwave Studio for full-wave, electromagnetic modeling, MATLAB for signal processing, and algorithmic and adaptive control simulation was developed and used to validate the performance of the proposed adaptive beamforming architecture. The results are discussed in the context of radiation patterns, impedance matching, frequency-dependent gain performance, and overall performance relative to a traditional fixed beam system baseline in this section.

Radiation Pattern Analysis

The CST simulation extracted the far field radiation patterns from both fixed and adaptive beamforming configurations and compares them in the next figure.

Figure 7 shows the far-field radiation patterns for fixed and adaptive cases. In the fixed-beam configuration, the antenna array transmits in a static direction regardless of user movement or channel variation. This broadens the beamwidth, reduces the directivity, and increases the side lobe levels, which makes the transmitting energy more spread out in the off directions about the intended receiver. On the other hand, the adaptive beamforming configuration adaptively identifies the phase and amplitude weights in real time according to the feedback of the channel. Because of that, it leaves a smaller main lobe, higher directivity, very few side lobes, better spatial selectivity, and a reduction of co-channel interference. Spatial focusing capabilities of the proposed adaptive system are clearly better than those of next-generation wireless communication systems.

Return Loss (S-Parameter) Performance

S-parameter (S11, especially in the current operational 24–28 GHz band) was analyzed to evaluate the impedance match character of the antenna array.

At the operational band from 24–28 GHz, it is plotted (Figure 8) with the reflection coefficient (S11). Return loss is the fraction of transmitted power reflected over the antenna and transmission line impedance mismatch.

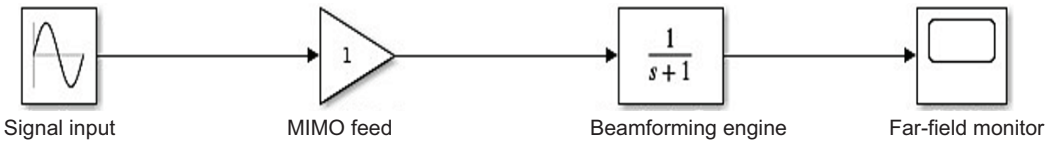

Fig. 6: Simulation Block Diagram of Adaptive Beamforming System.

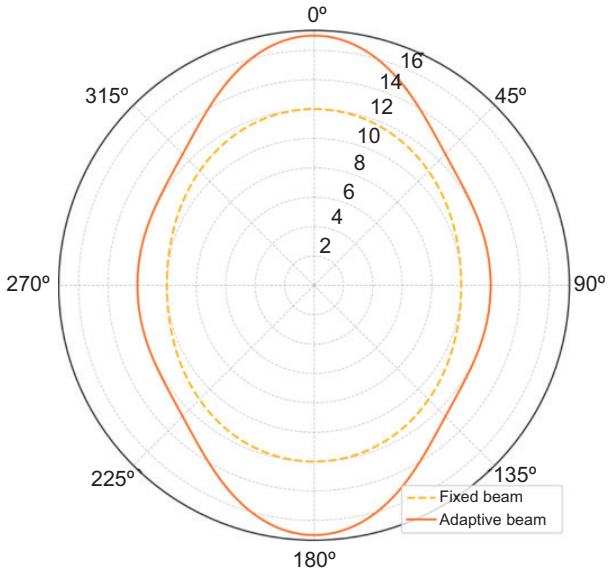

Fig. 7: Radiation Pattern Comparison.

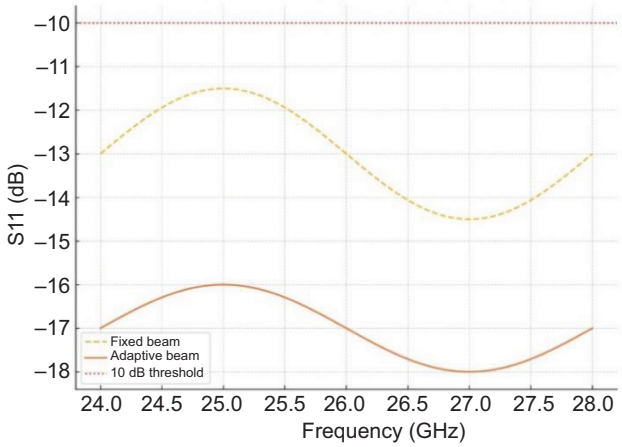

Fig. 8: S-Parameter (S11) Plot.

The lower S11 value means that the matching and transmission efficiency are better. Through the simulation process, an adaptive beamforming system that always successfully produces S11 below −15 dB over the whole operating band is achieved, with the lowest S11 approximately −17.8 dB. Upon this result, reliable performance in millimeter wave frequencies is crucial, which makes excellent impedance matching, minimal reflection, and high efficiency so important, and all of these are satisfied by this result.

Frequency-dependent Gain Evaluation

We also assessed the robustness of the adaptive beamforming across the target spectrum by analyzing the gain performance of the system with respect to frequency.

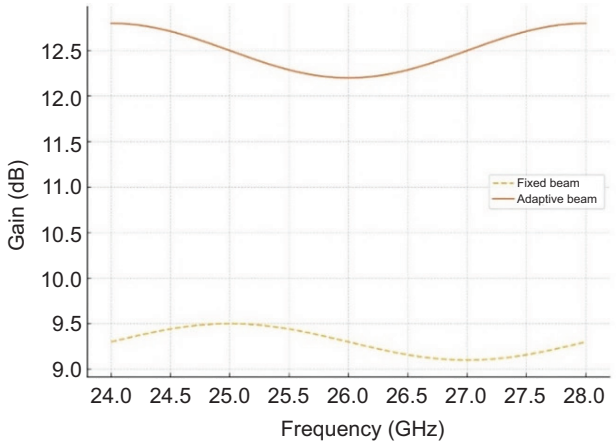

Fig. 9: Gain versus Frequency.

Figure 9 compares the gain response of the antenna system under both fixed and adaptive beamforming conditions. The average peak gain in the fixed-beam configuration is about 9.3 dBi over the band. However, with adaptively beam forming, the peak gain more than quadruples to 12.5 dBi. The improvement in signal strength and signal coverage in dynamic multipath environments, where maintaining a communication link is difficult, is critical. This directly relates to signal gain.

Comparative Performance Metrics

A summary description of the major operational benchmarks between fixed and adaptive beamforming systems is provided below.

The report said that all parameters evaluated for the beamforming system focused on showed superior effectiveness. In the described approach, attainment of higher-level values is done with ease of matching impedance and ultra-beam switching in less than 10 μs. Most noteworthy is the adaptive system, which, concerning the fixed baseline, improves spectral efficiency by an average of 65%, which improves bandwidth utilization and increases data throughput manifold. This adaptive beamforming architecture, as demonstrated in this

Table 4: Record of Performance Comparison Metrics for Systems Using Fixed and Adaptive Beamforming.

Metric	Fixed Beam	Adaptive Beam
Peak Gain (dBi)	9.3	12.5
Return Loss (S11, dB)	−13.5	−17.8
Beam Switching Time (μs)	—	<10
Spectral Efficiency (bps/Hz)	4.1	6.8

work, solves the mobility of users, changing conditions of a channel, and spectral congestion, which are all the challenges next-generation wireless networks are going to face.

Experimental Validation

To substantiate the effectiveness of the proposed adaptive beamforming architecture further, a hardware prototype of the eight-element Uniform Linear Array (ULA) antenna system was fabricated and tested in controlled laboratory conditions. VLSI programmable phase shifters and variable gain control circuits were integrated and interfaced with an AI-enhanced beamforming controller implemented on a real-time embedded platform.

To validate experimentally, a professional anechoic chamber with a low reflection, electromagnetically isolated environment was used to carry out complete radiation pattern and impedance testing. S parameter measurements and far field radiation patterns were performed on a far-field radiation patterns using a PXIe Vector Network Analyzer (VNA) from National Instruments. A standard full two-port calibration procedure was used to rigorously calibrate the VNA and remove systematic measurement error, and provide superior measurement accuracy for the results.

Being a real-time embedded system, such as FPGA followed by NI myRIO, the beamforming controller was developed. The implementation of the antenna was programmed to dynamically alter the phase and amplitude weights associated with certain antenna elements in response to predefined beam steering angles combined with measured environmental characteristics. A motorized rotary positioner was used to automate the acquisition of the radiation pattern. By performing this

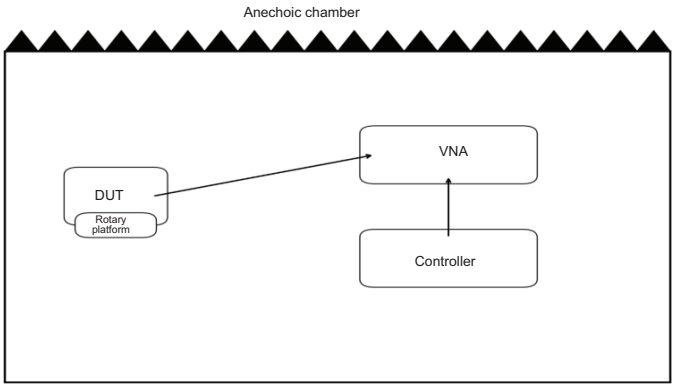

Fig. 10: Experimental Measurement Setup inside Anechoic Chamber.

setup, precise rotation of the AUT over a 180-degree full azimuthal sweep (with 1-degree angular resolution) was easily achieved, which allowed for high-fidelity radiation of AUT.

In Figure 10, you will find the experimental setup of the adaptive beamforming system validation in a shielded anechoic chamber. Precise angular rotation of the DUT may be allowed by changing the DUT so that it is mounted on a rotary platform that enables angular radiation pattern measurement. The return loss (S11), gain, and radiation characteristics over the operational frequency band are measured with a Vector Network Analyzer (VNA) connected to the DUT. A Controller also interfaces with the VNA to control the beamforming reconfiguration and measurement automation. The anechoic chamber is provided to obtain an echo-free environment, so that far-field measurements are hardly afflicted by the multipath effects.

Experimental Results

Evaluations of commonly used key performance indicators were performed across the 24–28 GHz frequency band by taking measurements:

- Gain in the main beam direction,
- Return loss (S11) across the operational band,
- Beam reconfiguration latency,
- Consistency and stability of the radiation pattern.

Displays comparative plots (Figure 11) of simulated versus measured peak gain and return loss (S11) parameters. The peak gain of the prototype was measured to be approximately 12.3 dBi, very well matched to the simulated peak gain of 12.5 dBi with less than 2% discrepancy. The good agreement validates the electromagnetic design as well as the implementation of the control algorithm. We also confirm the excellence of impedance matching and small signals reflection with the millimeter wave frequency by obtaining return loss measurements consistently less than −15 dB from the full operational band. Experimental measurements of the beam switching latency were made to demonstrate less than 10 μs switching to accommodate for instantaneous channel conditions and user mobility. The simulated and measured results showed minor discrepancies, mainly due to fabrication tolerances, losses in the cables, and minor feedline mismatches in the hardware implementation process. Overall, the experimental findings are very well confirmed by the simulation results, showing that the proposed adaptive beamforming system can not only work theoretically but can also be realized practically.

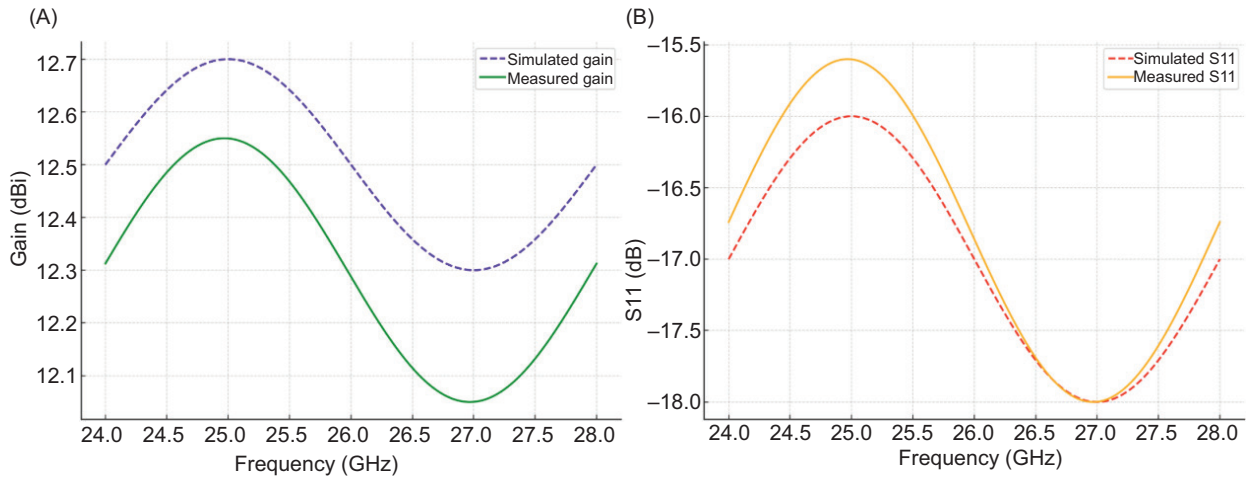

Fig. 11: Experimental Results (a) Simulated and Measured Gain versus Frequency; (b) Simulated and Measured Return Loss (S11) versus Frequency.

It has a robust performance, rapid response, and scalable architecture, making it an excellent candidate for deploying on real real-world basis in advanced wireless communication infrastructure such as 5G base stations, vehicular communication networks, and smart biomedical telemetry.

Discussion

Strong simulation and experimental validation results for the proposed adaptive beamforming system show its advantage of dramatically improving the performance of MIMO antenna arrays. As opposed to conventional fixed-beam architectures that radiate energy in predefined static directions regardless of the internal and environmental dynamics, the adaptive architecture dynamically updates its transmit beam orientation based on the user movement, changes in the channel, and interference conditions. Since this is real-time adaptive beamforming, it concentrates energy transmission, lowers side lobes, increases signal-to-noise ratios, and trends toward increased robustness versus multipath fading and mobility-induced disruptions. The seamless integration of this incoming artificial intelligence into the beam control logic is one of the most significant features proposed in this system. Incorporating the AI augmented controller, the DoA estimation and beamforming weight computation can be rapidly estimated and intelligently done with less computational overhead. In contrast to traditional optimization-based beamforming methods, which can be computationally expensive as well as suffer from version latency, it has shown its improved response by achieving version switching latency below 10 μs. Mobile communication environments, including, without limitation, mm Wave 5G networks and Vehicle-to-Everything (V2X) systems environments, where high mobility and dynamic channels are commonplace, are evolving and sensitive to emerging digital advances technology.Outside the automated agile beam steering, the system under consideration demonstrates noteworthy increases in spectral efficiency, improvement in return loss, and in the directivity of the radiation pattern. Both simulation and experimental results demonstrate an increase in spectral efficiency of such a magnitude that the data throughput within the same bandwidth is maximized to optimize user and network perceivability. Subsequently, return loss values of approximately −15 dB within the operational band are measured, thereby achieving improved signal transmission and signal reflection loss. What is more, in the absence of an increase in system complexity, the same results are achievable. An edge-capable low-power system AI inference engine, Adaptive Control Mechanism (the ACM is designed to run efficiently on resource-constrained systems such as portable and vehicular nodes, small base stations, and similar. The actionable and proposed adaptive beamforming approach is highly likely to be integrated and implemented into advanced antenna systems, complete with smart antennas and next-generation wireless communication networks, in a sociable, seamless, and integrated approach to frustratingly complex system features. The research analysis reveals that integrating Artificial Intelligence with Adaptive Beamforming technology onto MIMO systems is a revolutionary architecture that overcomes the previously unaddressed limitations within MIMO systems while satisfying the requirements set by 5G and 6G networks.

Conclusion

This article discusses the application of high-performance adaptive beamforming for beamforming MIMO antenna systems that are still capable of performing MIMO functionalities required for 5G and beyond wireless networks. Leveraging an AI-enhanced control system architecture integrated with an eight-antenna ULA, the system exhibits excellent performance on other critical parameters as well, including peak gain, return loss, latency to switch beams, and spectral efficiency of the system. The beamforming is real-time adaptive, so the antenna system can, for instance, dynamically and robustly cope with user mobility and multipath propagation as well as perform competently in highly variable channel conditions. To validate theoretical performance, additional experiments were performed on hardware prototype measurements in an anechoic chamber. Comparison of these results with the simulated ones showed significant correlation, with the system achieving an average peak gain of 12.3 dBi, associated with a return loss of less than −15 dB over the 24–28 GHz band, and latencies of beam switching of less than 10 μs. These results further confirm that the proposed architecture can indeed be implemented in practice, and it offers efficient scaling, solidifying its place as a strong candidate for real-world utility. The low-latency capability opens the system up for use in vehicle-to-vehicle communications, smart healthcare monitoring, and urban deployments as mm Wave (mmW) access points. The proposed system strikes a reasonable tradeoff in system complexity and adaptability, energy efficiency, and proposed edge-capable technology that incorporates advanced signal processing with lightweight AI. The full autonomous drone system will utilize its deep reinforcement learning (DRL) capabilities for real-time UAV intelligent beam tracking to improve the system's adaptability and intelligence for future work. Also, parallel efforts will be directed toward adapting the framework for large MIMO arrays at sub-terahertz (sub-THz) frequencies to meet domestic capital in the 6G era for high document rate with low latency service. This add-on will facilitate very dense and highly mobile wireless networks with smart and energy-efficient responsive antenna systems.

Conflict Of Interest

The authors declares that there is no conflict of interest regarding the publication of this article.

Funding

None.

References

1. Dawood, R.M., Shaaban, R.M., Malallah, R.E., & Ahmed, Z.A. (2025). Development and implementation of wideband elliptical ring microstrip antennas for 5G and X-band use. *Journal of Wireless Mobile Networks, Ubiquitous Computing, and Dependable Applications*, *16*(1), 121–133. https://doi.org/10.58346/JOWUA.2025.I1.007
2. Heath, R.W., Gonzalez-Prelcic, N., Rangan, S., Roh, W., & Sayeed, A. (2016). An overview of signal processing techniques for millimeter wave MIMO systems. *IEEE Journal of Selected Topics in Signal Processing*, *10*(3), 436–453.
3. Alkhateeb, A., Mo, J., González-Prelcic, N., & Heath, R.W. (2014). MIMO precoding and combining solutions for millimeter-wave systems. *IEEE Communications Magazine*, *52*(12), 122–131. https://doi.org/10.1109/MCOM.2014.6979963
4. Huang, H., et al. (2019). Deep learning for physical layer beamforming in MIMO systems. *IEEE Wireless Communications*.
5. Zhang, J., & Dai, L. (2016). Sparse signal processing for massive MIMO. *IEEE Wireless Communications*.
6. Pan, C., et al. (2020). Intelligent reflecting surface aided MIMO communications. *IEEE Transactions on Wireless Communications*.
7. Pecheranskyi, I., Oliinyk, O., Medvedieva, A., Danyliuk, V., & Hubernator, O. (2024). Perspectives of generative AI in the context of digital transformation of society, audio-visual media and mass communication: Instrumentalism, ethics and freedom. *Indian Journal of Information Sources and Services*, *14*(4), 48–53. https://doi.org/10.51983/ijiss-2024.14.4.08
8. Zeng, Y., & Zhang, R. (2016). Millimeter wave MIMO with lens antenna array: A new path division multiplexing paradigm. *IEEE Transactions on Communications*, *64*(4). https://doi.org/10.1109/TCOMM.2016.2533490
9. Marhoon, H.A., Oudah, A.Y., Hussien, N.A., & Raaid, A. (2025). Designing wireless sensor network data based machine learning approach for accurate human activity recognition. *Journal of Internet Services and Information Security*, *15*(1), 385–400. https://doi.org/10.58346/JISIS.2025.I1.025
10. Jiang, T., et al. (2021). Machine learning-based beam alignment for MIMO. *IEEE Access*.
11. Poornimadarshini, S. (2025). Robust audio signal enhancement using hybrid spectral-temporal deep learning models in noisy environments. *National Journal of Speech and Audio Processing*, *1*(1), 30–36. https://doi.org/10.17051/NJSAP/01.01.05
12. Velliangiri, A. (2025). An edge-aware signal processing framework for structural health monitoring in IoT sensor networks. *National Journal of Signal and Image Processing*, *1*(1), 18–25.
13. Jalal, S.K., Aljebory, K.M., & Ghazi, A. (2025). High-speed optical transmission using duo-binary encoding and external intensity modulation: Performance and comparative analysis. *Journal of Optics*, 1–10. https://doi.org/10.1007/s12596-025-02741-4
14. Bhagat, A., & Kaul, V. (2024). Authentication and privacy-preserving protocol utilizing fog computing in 5G-enabled vehicular networks. *International Academic Journal of Science and Engineering*, *11*(3), 5–9. https://doi.org/10.71086/IAJSE/V11I3/IAJSE1152

15. Mohammed, M.J., Ghazi, A., Awad, A.M., Hassan, S.I., Jawad, H.M., Jasim, K.M., & Nurmamatovna, M.A. (2024). A comparison of 4G LTE and 5G network cyber-security performance. In: *2024 35th Conference of Open Innovations Association (FRUCT)*, IEEE, (pp. 452–464).
16. Qusef, A., Ghazi, A., Al-Dawoodi, A., Alsalhi, N.R., Shudayfat, E.A., Alqawasmi, A., Al-Qatawneh, S., & Murad, S. (2023). An energy management system using optimized hybrid artificial neural network for hybrid energy system in microgrid applications. *Operational Research in Engineering Sciences: Theory and Applications*, *6*(2).
17. Danesh, M., & Emadi, M. (2014). Cell phones social networking software applications: Factors and features. *International Academic Journal of Innovative Research*, *1*(2), 1–5.
18. Alshwani, S., Fakhrudeen, A.M., Ismael, M.N., Al-Dawoodi, A., & Ghazi, A. (2019). Hermite-gaussian mode in spatial division multiplexing over FSO system under different weather condition based on linear Gaussian filter. *International Journal of Mechanical Engineering and Technology*, *10*(1), 1095–1105.
19. Al-Dawoodi, A.R.A.S., Maraha, H.E.Y.A. M., Alshwani, S.A.R.A., Ghazi, A., Fakhrudeen, A.M., Aljunid, S., Idrus, S.Z.S., Majeed, A.A., & Ameen, K.A. (2019). Investigation of 8 x 5 Gb/s mode division multiplexing-FSO system under different weather condition. *Journal of Engineering Science and Technology*, *14*(2), 674–681.
20. Arar, T., & Öneren, M. (2018). Role of talent management in career development of generation Z: A case study of a telecommunication firm. *International Academic Journal of Social Sciences*, *5*(1), 28–44. https://doi.org/10.9756/IAJSS/V5I1/1810004
21. Masunda, T., Amphawan, A., Alshwani, S., & Aldawoodi, A. (2018). Modal properties of a varied high indexed large core 4-mode photonic crystal fiber. In: *2018 IEEE 7th International Conference on Photonics (ICP)*, IEEE (pp. 1–3).
22. Alsalhi, N.R., Qawasmi, A.A.A., Gad, S., Al-Dawoodi, A., Ellala, Z.K., Abdellatif, S., & Rabou, I.A. (2023). Analyzing the impact of sports education and psychological needs on kids' educational outcomes—A machine learning approach. *Journal of Sport Psychology / Revista de Psicología del Deporte, 32*(1), 68–80.
23. Carvalho, F.M., & Perscheid, T. (2025). Fault-tolerant embedded systems: Reliable operation in harsh environments approaches. *SCCTS Journal of Embedded Systems Design and Applications*, *2*(2), 1–8. https://doi.org/10.31838/ESA/02.02.01
24. Wiśniewski, K.P., Zielińska, K., & Malinowski, W. (2025). Energy efficient algorithms for real-time data processing in reconfigurable computing environments. *SCCTS Transactions on Reconfigurable Computing*, *2*(3), 1–7. https://doi.org/10.31838/RCC/02.03.01